

# Predictive Effective Mobility Model for FDSOI Transistors using Technology Parameters

Pragya Kushwaha, Harshit Agarwal, Mandar Bhoir and Nihar R. Mohapatra  
 Yogesh S. Chauhan  
 Indian Institute of Technology Kanpur  
 Kanpur, India  
 Email: kpragya@iitk.ac.in

Indian Institute of Technology Gandhinagar  
 Gandhinagar, India

Sourabh Khandelwal  
 Juan P. Duarte, Yen-Kai Lin  
 Huan-Lin Chang and Chenming Hu  
 University of California Berkeley  
 Berkeley, USA

**Abstract**—The formulation of effective mobility for fully depleted silicon-on-insulator (FDSOI) transistors is a very challenging task. As vertical electric field ( $E_{eff}$ ) changes its sign from positive to negative according to the front and back channel dominance which results in non-unique relationship between  $E_{eff}$  and carrier distribution. This is the first time, when a predictive mobility model for wide range of back gate biases, solely dependent on technology parameters (front and back gate oxide thickness  $T_{ox/box}$ , threshold voltage  $V_{th}$ , front/back gate bias  $V_{fg/bg}$  and flat-band voltage  $V_{fb}$ ) is proposed. This predictive mobility model allows the user to predict the deviation in device characteristics due to the variations in the device structure.

**Index Terms**—FDSOI, Model, Split-CV, Mobility.

## I. INTRODUCTION

Below 20 nm technology node, bulk transistors are facing challenges like severe short channel effects, random dopant fluctuation etc [1]. Different architectures like fully depleted silicon on insulator (FDSOI) [2] and FinFETs [3] are introduced to drive the CMOS market further for meeting high performance and low power demands. Due to the presence of ultra thin buried oxide layer (BOX), FDSOI transistor has threshold voltage tuning facility by back gate biasing [4]–[7] in comparison to FinFET transistors. This also results in strong front and back gate coupling which makes the effective electric field [8] and inversion layer mobility [9] calculations difficult in FDSOI transistors as compared to bulk transistors.

In bulk transistor, the inversion layer mobility follows a universal relation and is independent of substrate bias, the substrate doping and oxide thickness when plotted against effective transverse electric field  $E_{eff(bulk)}$  [10],

$$E_{eff(bulk)} = \frac{Q_{dep} + \eta Q_{inv}}{\epsilon_{Si}} \quad (1)$$

where  $Q_{dep}$ ,  $Q_{inv}$  are the depletion and inversion charges respectively,  $\epsilon_{Si}$  is the relative permittivity of silicon and  $\eta$  is 1/2 for nMOS and 1/3 for pMOS transistors. This universal mobility curve (UMC) is considered as a reference curve to compare any new technology and is very useful to understand the MOS transistor physics [8].

Unfortunately, the same definition of  $E_{eff(bulk)}$  is not applicable to the FDSOI transistors because electric field at the back interface ( $E_{sb}$ ) is not always equal to zero as in bulk MOS transistor [11]. This had led to lots of discussion on the

non-universality of mobility in literature [8], [12], highlighting the importance of  $E_{sb}$ . To account the impact of  $E_{sb}$  on mobility, the models proposed till date [13]–[15] have tried to include back gate electric field  $E_{sb}$  along with the front-gate electric field  $E_{sf}$  which results in effective electric field  $E_{eff} = \frac{Q_b + \eta Q_{inv}}{\epsilon_{Si}} + E_{sb}$ . Unfortunately, the lumped parameter  $E_{eff}$  is not a convenient quantity to use, when expressed in terms of  $Q_b$  and  $Q_{inv}$  [11], [15] as their measurements are difficult [16]. In this work, we have proposed a complete technology parameter based compact model for  $E_{eff}$  and effective mobility  $\mu_{eff}$ . Due to some manufacturing variations, technology parameters ( $T_{ox/box}$ ,  $V_{th}$ ,  $V_{fg/bg}$ ,  $V_{fb}$ ) show slight device to device variations. Also devices fabricated using different processes have different technology parameters. All these result in deviation of mobility and hence the device characteristics. The proposed predictive model captures these variations and predicts the effective mobility for wide range of back bias.

This paper is organized as follows. The mobility and threshold voltage extraction are explained in Section II. The proposed effective mobility model is discussed in Section III. Model validation is discussed in Section IV followed by conclusion in Section V.

## II. MOBILITY AND THRESHOLD VOLTAGE EXTRACTION

FDSOI devices from CEA-LETI were used for C-V and I-V measurements. The device chosen for this work has dimensions: channel length  $L_g = 10 \mu\text{m}$ , channel width  $W_g = 50 \mu\text{m}$  and front-gate oxide thickness  $T_{ox} = 1.2 \text{ nm}$ , back gate oxide thickness  $T_{box} = 25 \text{ nm}$  and silicon channel thickness  $T_{Si} = 8 \text{ nm}$ . I-V and C-V measurements are done using Keysights B1500A semiconductor device parameter analyzer. I-V measurements are done at drain voltage ( $V_{ds}$ ) = 10 mV while C-V measurements are done at  $V_{ds} = 0 \text{ V}$ .

### A. Mobility Extraction by Split-CV method

Fig. 1(a) shows the variation in gate to channel capacitance ( $C_{gc}$ ) as a function of  $V_{fg}$  for different  $V_{bg}$ . For high positive  $V_{bg}$  (i.e., Region-I), there is a plateau in  $C_{gc} - V_{fg}$  characteristic. This plateau indicates the formation of inversion layer at back side channel while there is no channel formed yet at the front interface [17], [18]. In region II, the front gate voltage

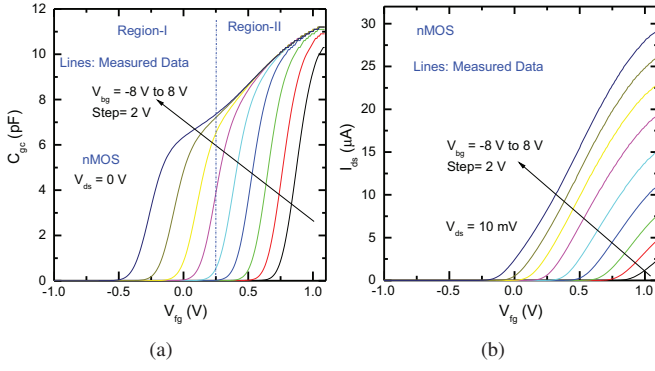


Fig. 1. The impact of back gate bias on measured  $C_{gc}$  and  $I_{ds}$  is illustrated. (a)  $C_{gc}$  vs  $V_{fg}$  characteristic. (b)  $I_{ds}$  vs  $V_{fg}$  characteristic. Back gate bias  $V_{bg}$  sweeps from -8 to 8 V with the step size of 2 V. Device dimensions are:  $L_g = 10 \mu\text{m}$ ,  $W_g = 50 \mu\text{m}$ ,  $T_{ox} = 1.2 \text{ nm}$ ,  $T_{box} = 25 \text{ nm}$ ,  $T_{Si} = 8 \text{ nm}$ . All lines are showing measurement data.

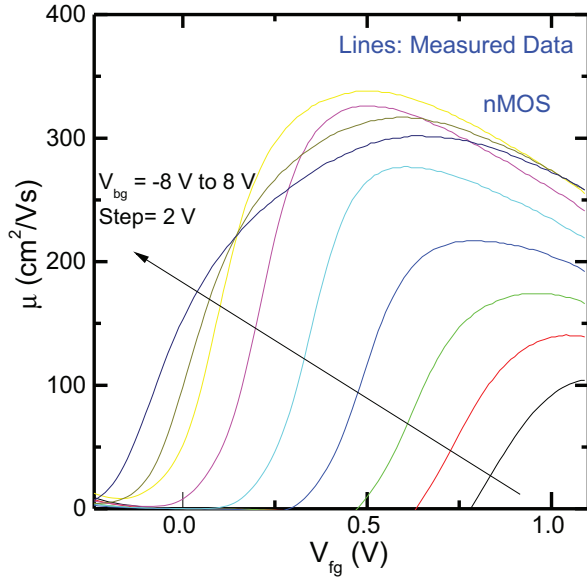


Fig. 2. Mobility  $\mu$  vs  $V_{fg}$  curve, by using definition (2). Device dimensions are:  $L_g = 10 \mu\text{m}$ ,  $W_g = 50 \mu\text{m}$ ,  $T_{ox} = 1.2 \text{ nm}$ ,  $T_{box} = 25 \text{ nm}$ ,  $T_{Si} = 8 \text{ nm}$ . All lines are showing measurement data.

is high, which results in coexistence of front as well as back channel inversion [19]. Fig. 1(b) shows the variation in drain current  $I_{ds}$  with  $V_{fg}$  for different  $V_{bg}$ . As  $V_{bg}$  increases,  $V_{th}$  of device decreases which results in high  $I_{ds}$  while with negative  $V_{bg}$ , inversion gets delayed and result in reduced  $I_{ds}$  [20].

The split C-V method is widely used for determining the mobility, because it estimates carrier density accurately [10]. Using this approach, the channel mobility is extracted using the  $C_{gc}$  vs  $V_{fg}$  characteristic and drain current measurements at different back gate biases [17] as follows

$$\mu = \frac{L_{eff} I_{ds}}{W_{eff} Q_{inv} V_{ds}} \quad (2)$$

where  $W_{eff}$ ,  $L_{eff}$  are the channel width and length respec-

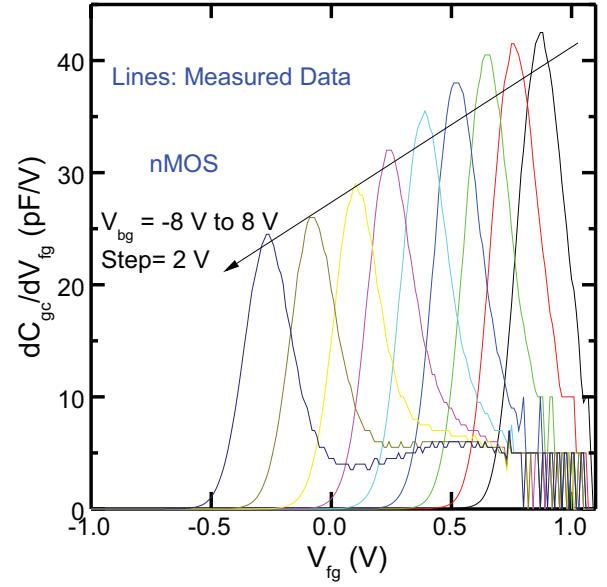


Fig. 3.  $\frac{dC_{gc}}{dV_{fg}}$  vs  $V_{fg}$  for different  $V_{bg}$  is illustrated. Device dimensions are:  $L_g = 10 \mu\text{m}$ ,  $W_g = 50 \mu\text{m}$ ,  $T_{ox} = 1.2 \text{ nm}$ ,  $T_{box} = 25 \text{ nm}$ ,  $T_{Si} = 8 \text{ nm}$ . All lines are showing measurement data.

tively and  $C_{ox}$  is front gate oxide capacitance.  $Q_{inv}$  is the charge per unit area which is obtained by integrating the measured  $C_{gc} - V_{fg}$  characteristic.

To neglect the effect of horizontal electric field on channel mobility, the measurements were carried out at  $V_{ds} = 10 \text{ mV}$ . Also the mobility curves were corrected for access resistance  $R_{access} = 2 * 10^3 \Omega \cdot \mu\text{m}$ , calculated using  $R_{on}(L)$  method [21]. The corrected mobility curves show that the  $R_{access}$  has negligible effect due to the use of long channel length device. The extracted  $\mu$  vs  $V_{fg}$  characteristic for different back gate bias are shown in Fig 2.

### B. Threshold Voltage Extraction

Fig. 1(b) shows that back-gate bias has a significant influence on  $V_{th}$ , thus it is important to extract  $V_{th}$  accurately. There are several methods available in literature to extract threshold voltage of MOS transistors [22], [23]. The derivative of the gate to channel capacitance method (see Fig 3) gives much better resolution in channel separation, because it is less sensitive to series resistance as compared to the current measurements. Extracted threshold voltage from the peak of the  $\frac{dC_{gc}}{dV_{fg}}$  curve is shown in Fig 4.

### III. PROPOSED EFFECTIVE MOBILITY MODEL

In a FDSOI transistor, the two boundary conditions from Gauss law at front and back gates are given as

$$\epsilon_{si} E_{sf} = Q_f = \frac{\epsilon_{ox}}{T_{ox}} (V_{fg} - V_{fb1} - \psi_1) \quad (3)$$

$$\epsilon_{si} E_{sb} = Q_b = \frac{\epsilon_{ox}}{T_{box}} (V_{bg} - V_{fb2} - \psi_2) \quad (4)$$

where  $Q_f$  and  $Q_b$  are the front/back gate charges and  $\epsilon_{si}$  and  $\epsilon_{ox}$  are the silicon and oxide material permittivity, respectively.

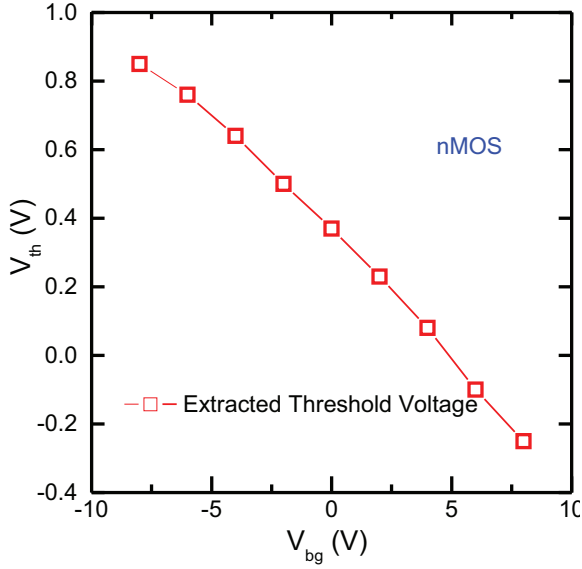


Fig. 4.  $V_{th}$  vs  $V_{bg}$  curve extracted from  $\frac{dC_{gc}}{dV_{fg}}$  vs  $V_{fg}$  characteristic. Device dimensions are:  $L_g = 10 \mu\text{m}$ ,  $W_g = 50 \mu\text{m}$ ,  $T_{ox} = 1.2 \text{ nm}$ ,  $T_{box} = 25 \text{ nm}$ ,  $T_{Si} = 8 \text{ nm}$ .

$V_{fb1}$  and  $V_{fb2}$  are the flat band voltages,  $T_{ox}$  and  $T_{box}$  are the oxide thicknesses at front and back gates, respectively.  $E_{sf}$  and  $E_{sb}$  are the surface electric fields and  $\psi_1$  and  $\psi_2$  are the surface potentials at front and back gates, respectively.

$$E_{sf} = \frac{V_{fg} - V_{fb1} - \psi_1}{3T_{ox}} \quad (5)$$

$$E_{sb} = \frac{V_{bg} - V_{fb2} - \psi_2}{3T_{box}} \quad (6)$$

We have assumed  $\psi_1 = \psi_2 = 2\phi_f$  i.e., threshold condition, where  $\phi_f$  is the Fermi potential. Effective mobility ( $\mu_{eff}$ ) can be expressed as a function of  $E_{eff}$  (i.e., average of front and back surface electric fields). Using (5) and (6),  $E_{eff}$  becomes

$$\begin{aligned} E_{eff} &= \frac{1}{6T_{ox}} \left[ (V_{fg} - V_{fb} - 2\phi_f) - \frac{T_{ox}}{T_{box}} (V_{bg} - V_{fb} - 2\phi_f) \right] \\ &= \frac{1}{6T_{ox}} \left[ V_{fg} - \frac{T_{ox}}{T_{box}} V_{bg} - \left(1 - \frac{T_{ox}}{T_{box}}\right) (V_{fb} + 2\phi_f) \right] \end{aligned} \quad (7)$$

where  $V_{fb1} = V_{fb2} = V_{fb}$  for derivation simplicity. In thin BOX FDSOI transistors, the technological variations at the back interface like oxide thickness, interface quality and work-function plays an important role. We have expressed  $V_{bg}$  in terms of threshold voltage  $V_{th}$  which automatically captures all these process variations in our model [24]. This relation also helps in capturing the effect of back bias on carrier distribution which makes effective mobility curves, nearly independent of back gate bias. As shown in Fig. 4,  $V_{th}$  can be expressed as

$$V_{th} = -\mathbf{m}V_{bg} + V_{th0} \quad (8)$$

where  $\mathbf{m}$  is representing the slope and  $V_{th0}$  is the threshold voltage at zero back gate bias. By incorporating (8) in (7), we

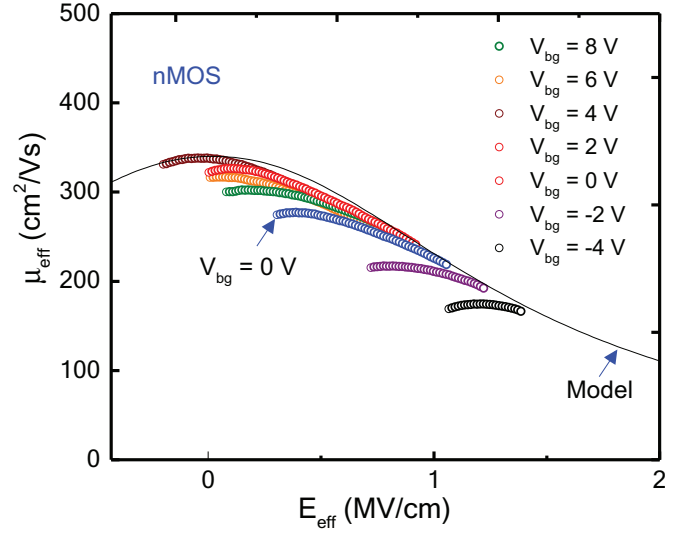


Fig. 5.  $\mu_{eff}$  vs  $E_{eff}$  behavior of FDSOI transistor is illustrated. Here,  $\alpha = 0.72$  and  $\beta = 1.1$ ,  $\mathbf{U0} = 380 \text{ cm}^2/\text{Vs}$ ,  $\mathbf{UA} = 0.83 \text{ cm/MV}$  and  $\mathbf{EU} = 1.85$ . Device dimensions are:  $L_g = 10 \mu\text{m}$ ,  $W_g = 50 \mu\text{m}$ ,  $T_{ox} = 1.2 \text{ nm}$ ,  $T_{box} = 25 \text{ nm}$ ,  $T_{Si} = 8 \text{ nm}$ . Black solid line: Predictive Model, Symbols: Measurement Data.

get final expression for  $E_{eff}$  as,

$$\begin{aligned} E_{eff} &= \frac{1}{6T_{ox}} \left[ V_{fg} + \frac{T_{ox}}{mT_{box}} V'_{th} - \left(1 - \frac{T_{ox}}{T_{box}}\right) (V_{fb} + 2\phi_f) \right] \\ &= \frac{1}{6T_{ox}} \left[ V_{fg} + \alpha V'_{th} - \beta (V_{fb} + 2\phi_f) \right] \end{aligned} \quad (9)$$

where  $V'_{th} = |V_{th}| - V_{th0}$  and  $\alpha = \frac{T_{ox}}{mT_{box}}$ ,  $\beta = \left(1 - \frac{T_{ox}}{T_{box}}\right)$ . Here,  $\alpha$  and  $\beta$  are taken as model parameters. To account for different  $V_{fb1}$  and  $V_{fb2}$  conditions,  $\beta$  can be tuned further.

#### IV. MODEL VALIDATION

The results for mobility discussed in Section II plotted by our proposed model are shown in Fig 5.  $E_{eff}$  is negative for  $V_{bg} > 0 \text{ V}$  and as  $V_{fg}$  increases, the charge centroid shifts from the back interface to the front interface and  $E_{eff}$  changes its sign from negative to positive. In strong inversion region, the effective mobility curves are converging into the single curve. This single mobility curve is predicted using our effective mobility model where  $\mu_{eff}$  is a function of proposed  $E_{eff}$  as (10). The solid black line shown in Fig 5 is predicting the effective mobility behavior for different back bias.

$$\mu_{eff} = \frac{\mathbf{U0}}{1 + \mathbf{UA} \cdot |E_{eff}|^{\mathbf{EU}}} \quad (10)$$

where  $E_{eff}$  is electric field in MV/cm.  $\mathbf{U0}$  is low field mobility parameter while  $\mathbf{UA}$  and  $\mathbf{EU}$  parameters are used to capture surface roughness scattering [25]. When amount of inversion charge is lower in the channel, mobility gets limited by coulomb scattering [26]. Note that our model does not consider the coulomb scattering.

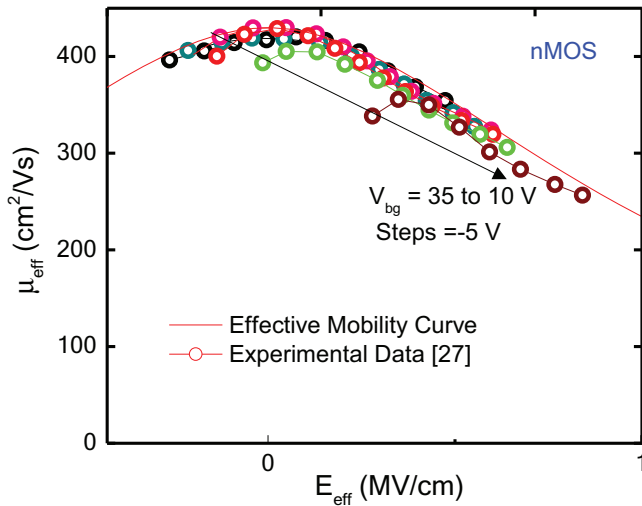


Fig. 6.  $\mu_{eff}$  vs  $E_{eff}$  behavior of FDSOI transistor. Device dimensions are:  $L_g = 10 \mu\text{m}$ ,  $W_g = 10 \mu\text{m}$ ,  $T_{ox} = 1.75 \text{ nm}$ ,  $T_{box} = 145 \text{ nm}$ ,  $T_{Si} = 11 \text{ nm}$ . Red solid line: Predictive Model, Symbols: Experimental Data [27].

To check the model validity for FDSOI transistors with different set of technology parameters ( $T_{ox}$ ,  $T_{box}$  and  $T_{Si}$ ), we have plotted proposed  $\mu_{eff}$  vs  $E_{eff}$  for the experimental data obtained from [27]. The model shows good agreement for this thick BOX FDSOI transistor for a wide range of back bias as shown in Fig 6. The proposed model is able to predict the mobility for differently processed FDSOI transistors as shown in Fig 5 and Fig 6. These results also show that the inclusion of threshold voltage in our model makes mobility curves independent of back bias.

## V. CONCLUSION

The predictive mobility model for FDSOI transistors is presented for a wide range of back gate bias. Model has shown good agreement with the measured data obtained from CEAL-LETI as well as with the data reported earlier in literature. The novelty in the proposed model is its dependency, solely on technology parameters which are monitored daily in the practical engineering world by circuit designers.

## VI. ACKNOWLEDGEMENT

This work was supported in part by Semiconductor Research Corporation, in part by Science and Engineering Research Board (SERB), in part by Ramanujan Fellowship and in part by Council of Scientific and Industrial Research (CSIR).

## REFERENCES

- [1] S. Markov *et al.*, "Statistical variability in scaled generations of n-channel UTB-FD-SOI MOSFETs under the influence of RDF, LER, OTF and MGG," in *Proc. of SOI Conference*, pp. 1-2, 2012.
- [2] X. Qian *et al.*, "Comprehensive Analysis of Short-Channel Effects in Ultrathin SOI MOSFETs," *IEEE Transactions on Electron Devices*, vol. 60, no. 6, pp. 1814-1819, 2013.
- [3] E. Amat *et al.*, "Impact of FinFET and III-V/Ge technology on logic and memory cell behavior," *IEEE Transactions on Device and Materials Reliability*, vol. 14, no. 1, pp. 344 - 350, 2014.

- [4] O. Nier *et al.*, "Efficient multi-Vt FDSOI technology with UTBOX for low power circuit design," in *Proc. of IEEE Symposium on VLSI Technology Digest of Technical Papers*, pp. 65-66, 2010.
- [5] C. Navarro *et al.*, "Multibranch Mobility Analysis for the characterization of FDSOI Transistors," *IEEE Electron Device Letters*, vol. 33, no. 8, pp. 1102-1104, 2012.
- [6] C. Sampedro *et al.*, "Reaching sub-32 nm nodes: ET-FDSOI and BOX optimization," *Solid-State Electronics*, vol. 70, pp. 101-105, 2012.
- [7] C. Fenouillet-Beranger *et al.*, "Impact of local back biasing on performance in hybrid FDSOI/bulk high-k/metal gate low power (LP) technology," *Solid-State Electronics*, vol. 88, pp. 15-20, 2013.
- [8] S. Cristoloveanu *et al.*, "Why the universal mobility is not," *IEEE Transactions on Electron Devices*, vol. 57, no. 6, pp. 1327-1333, June 2010.
- [9] A. Ohata *et al.*, "Impact of back-gate biasing on effective field and mobility in ultrathin silicon-on-insulator metal-oxide-semiconductor field-effect-transistors," *Journal of Applied Physics*, vol. 113, p. 144514, 2013.
- [10] S. Takagi *et al.*, "On the universality of inversion layer mobility in Si MOSFET's: Part I-effects of substrate impurity concentration," *IEEE Transactions on Electron Devices*, vol. 41, no. 12, pp. 2357-2362, Dec 1994.
- [11] H. Yoshimoto *et al.*, "Extension of universal mobility curve to multi-gate MOSFETs," in *IEEE International Electron Devices Meeting*, Dec 2007, pp. 703-706.
- [12] C. Navarro *et al.*, "Multibranch mobility analysis for the characterization of FDSOI transistors," *IEEE Electron Device Letters*, vol. 33, no. 8, pp. 1102-1104, 2012.
- [13] M. Sherony *et al.*, "SOI MOSFET effective channel mobility," *IEEE Transactions on Electron Devices*, vol. 41, no. 2, pp. 276-278, 1994.
- [14] H. Zenitani *et al.*, "Mobility model for advanced SOI-MOSFETs including back-gate contribution," *Japanese Journal of Applied Physics*, vol. 54, no. 4S, p. 04DC03, 2015.
- [15] O. Nier *et al.*, "Effective field and universal mobility in high-k metal gate UTBB-FDSOI devices," in *Proc. of International Conference on Microelectronic Test Structures (ICMTS)*, pp. 8-13, 2014.
- [16] K. Chen, "Analytical and compact models (BSIM3v3) for deep submicron CMOS," *Thesis, University of California, Berkeley*, 1998.
- [17] D. Esseni *et al.*, "An experimental study of mobility enhancement in ultrathin SOI transistors operated in double-gate mode," *IEEE Transactions on Electron Devices*, vol. 50, no. 3, pp. 802-808, March 2003.
- [18] A. Ohata *et al.*, "Mobility comparison between front and back channels in ultra-thin silicon-on-insulator transistors by the front-gate split capacitance-voltage method," *Appl Phys Lett*, vol. 89, 2006.
- [19] C. Jian *et al.*, "Threshold voltage and C-V characteristics of SOI MOSFET's related to Si film thickness variation on SIMOX wafers," *IEEE Transactions on Electron Devices*, vol. 39, no. 10, pp. 2346-2353, 1992.
- [20] C. Fenouillet-Beranger *et al.*, "Efficient multi-VT FDSOI technology with UTBOX for low power circuit design," in *Proc. of IEEE Symposium on VLSI Technology*, pp. 65-66, 2010.
- [21] B. Sheu *et al.*, "A capacitance method to determine channel lengths for conventional and LDD MOSFET's," *IEEE Electron Device Letters*, vol. 5, no. 11, pp. 491-493, 1984.
- [22] A. Ortiz-Conde *et al.*, "A review of recent MOSFET threshold voltage extraction methods," *Microelectronics Reliability*, vol. 42, no. 4-5, pp. 583 - 596, 2002.
- [23] H. Agarwal *et al.*, "Analytical modeling and experimental validation of threshold voltage in BSIM6 MOSFET model," *IEEE Journal of Electron Devices Society*, vol. 3, no. 3, pp. 240 - 243, 2015.
- [24] P. Kushwaha *et al.*, "Modeling the impact of substrate depletion in FDSOI MOSFETs," *Solid-State Electronics*, vol. 104, no. 0, pp. 6 - 11, 2015.
- [25] K. Chain *et al.*, "A MOSFET electron mobility model of wide temperature range (77-400 k) for IC simulation," *Semiconductor Science and Technology*, vol. 12, no. 4, p. 355, 1997.
- [26] Y. Tsidividis, *Operation and Modeling of the MOS Transistor*, 2013. Oxford, 2013.
- [27] T. Rudenko *et al.*, "Experimental study of transconductance and mobility behaviors in ultra-thin SOI MOSFETs with standard and thin buried oxides," *Solid-State Electronics*, vol. 54, no. 2, pp. 164 - 170, 2010.